

Chapter 7 : Uncertainty Analysis

After the velocity data acquired from the calibration wheel had been reduced, an uncertainty analysis was performed to determine the uncertainty of the velocities measured by the VT DGV system. All of the uncertainties discussed in this chapter have a confidence level of 95%. In addition to determining the overall uncertainty of the data obtained from the calibration wheel, this analysis was used to determine what factors in the acquisition and reduction of the calibration wheel data led to the largest increases in uncertainty. Determining what factors led to the largest increases in uncertainty will provide guidance on what portions of the VT DGV system will require the most attention to improve the performance of this system in the future.

The software used to calculate the standard deviations in the pixel intensities for a series of data images, the uncertainties of the reference value of the laser reference transmission ratio, the uncertainty of the laser reference transmission ratio and the uncertainty of the average reference transmission ratio for camera module i , was written by Troy Jones as part of his M.S. thesis.¹⁰⁷ The rest of the software used in this uncertainty analysis was written as part of this research. The procedure used to conduct this analysis was adapted from one discussed in Troy Jones' M.S. thesis.¹⁰⁸ The procedures used to calculate the uncertainty in the wave number used to reduce the calibration wheel velocity data and to calculate the uncertainty in the Euler angles used to determine the laser propagation vector were added to the procedure discussed in Jones' thesis. While this uncertainty analysis was being performed, errors in the procedures used to calculate the uncertainty of the transmission ratios used in the data reduction procedure were located and corrected

The governing equation used to solve for velocities in the DGV technique can be expressed in the following manner:

$$\begin{Bmatrix} V_x \\ V_y \\ V_z \end{Bmatrix} = \frac{c}{\nu_o} \begin{bmatrix} \sin\theta_{y1} + \sin\theta_{ylas} & -\sin\theta_{x1} \cos\theta_{y1} - \sin\theta_{xlas} \cos\theta_{ylas} & -\cos\theta_{x1} \cos\theta_{y1} - \cos\theta_{xlas} \cos\theta_{ylas} \\ \sin\theta_{y2} + \sin\theta_{ylas} & -\sin\theta_{x2} \cos\theta_{y2} - \sin\theta_{xlas} \cos\theta_{ylas} & -\cos\theta_{x2} \cos\theta_{y2} - \cos\theta_{xlas} \cos\theta_{ylas} \\ \sin\theta_{x3} + \sin\theta_{ylas} & -\sin\theta_{x3} \cos\theta_{y3} - \sin\theta_{xlas} \cos\theta_{ylas} & -\cos\theta_{x3} \cos\theta_{y3} - \cos\theta_{xlas} \cos\theta_{ylas} \end{bmatrix}^{-1} \begin{Bmatrix} \Delta\nu_1 \\ \Delta\nu_2 \\ \Delta\nu_3 \end{Bmatrix} \quad (51)$$

where V_x , V_y , and V_z were the velocity components in the x, y, and z directions, respectively, c was the speed of light, ν_o was the optical frequency of the laser pulse used to acquire DGV data, θ_{x1} , θ_{x2} , and θ_{x3} were the Euler angles, about the x axis, used to calculate the unit vector pointing toward the direction from which the data area is being viewed by camera modules 1, 2, and 3 respectively, θ_{y1} , θ_{y2} , and θ_{y3} were the Euler angles, about the y axis, used to calculate the unit vector pointing toward the direction from which the data area is being viewed by camera modules 1, 2, and 3 respectively, θ_{xlas} and θ_{ylas} were the Euler angles about the x and y axes, respectively, used to calculate the laser propagation unit vector, and $\Delta\nu_1$, $\Delta\nu_2$, and $\Delta\nu_3$ were the changes in optical frequency measured by camera modules 1, 2, and 3 respectively. Therefore, the general equation used to calculate the uncertainty of the velocity data was:

$$\omega V_j = \sqrt{\begin{aligned} & \left(\omega \Delta f_1 \cdot \frac{\partial V_j}{\partial \Delta \nu_1} \right)^2 + \left(\omega \Delta f_2 \cdot \frac{\partial V_j}{\partial \Delta \nu_2} \right)^2 + \left(\omega \Delta f_3 \cdot \frac{\partial V_j}{\partial \Delta \nu_3} \right)^2 + \\ & \left(\omega \theta_{x1} \cdot \frac{\partial V_j}{\partial \theta_{x1}} \right)^2 + \left(\omega \theta_{x2} \cdot \frac{\partial V_j}{\partial \theta_{x2}} \right)^2 + \left(\omega \theta_{x3} \cdot \frac{\partial V_j}{\partial \theta_{x3}} \right)^2 + \\ & \left(\omega \theta_{y1} \cdot \frac{\partial V_j}{\partial \theta_{y1}} \right)^2 + \left(\omega \theta_{y2} \cdot \frac{\partial V_j}{\partial \theta_{y2}} \right)^2 + \left(\omega \theta_{y3} \cdot \frac{\partial V_j}{\partial \theta_{y3}} \right)^2 + \\ & \left(\omega \theta_{xlas} \cdot \frac{\partial V_j}{\partial \theta_{xlas}} \right)^2 + \left(\omega \theta_{ylas} \cdot \frac{\partial V_j}{\partial \theta_{ylas}} \right)^2 + \left(\omega WN \cdot \frac{\partial V_j}{\partial WN} \right)^2 \end{aligned}} \quad (52)$$

where ωV_j was the uncertainty of the j^{th} velocity component, $\omega \Delta \nu_1$, $\omega \Delta \nu_2$, and $\omega \Delta \nu_3$ were the uncertainties in the change in optical frequency due to the Doppler effect, $\omega \theta_{x1}$, $\omega \theta_{x2}$, and $\omega \theta_{x3}$

were the uncertainties in the Euler angles about the x axis for the camera viewing angles, $\omega\theta_{y1}$, $\omega\theta_{y2}$, and $\omega\theta_{y3}$ were the uncertainties in the Euler angles about the y axis for the camera viewing angles, and $\omega\theta_{xlas}$, and $\omega\theta_{ylas}$ were the uncertainties in the Euler angles used to calculate the laser propagation vector. The term ωWN was the uncertainty in the calculated wave number of the laser pulse. As was discussed in Chapter 2, the wave number was defined to be ν_o / c . The uncertainty of each velocity component (V_x , V_y , and V_z) was calculated at each pixel location in the data plane. The average uncertainty for each of these velocity components was also calculated.

7.1 Calculating Frequency Shift Uncertainties

Before the uncertainty of the acquired velocities could be calculated, the uncertainties on the right hand side of equation 52 had to be determined. The frequency shift uncertainties: $\omega\Delta\nu_1$, $\omega\Delta\nu_2$, and $\omega\Delta\nu_3$, will be considered first. The change in optical frequency due to the Doppler effect was determined by calculating the difference in the optical frequency at each pixel location in the data plane and the optical frequency of the unshifted laser beam. Both optical frequencies were calculated using the frequency calibration functions contained in equations 47 through 49. These three equations were functions of transmission ratio and so the change in optical frequency was a function of transmission ratio, as can be seen in equation 53:

$$\Delta\nu_i = \nu_i(TR_i) - \nu_i(TR_i^{ref}) \quad (53)$$

where $\nu_i(TR_i)$ was the frequency calibration function for camera module i , solved at each pixel location in the data plane, and $\nu_i(TR_i^{ref})$ was the frequency calibration function solved using the laser reference transmission ratio calculated for the camera module as described in section 4.6.3. From equation 53, the equation to express the uncertainty of $\Delta\nu_i$ was derived to be:

$$\omega\Delta\nu_i = \sqrt{\left(\omega TR_i \cdot \frac{\partial\Delta\nu_i}{\partial TR_i}\right)^2 + \left(\omega TR_i^{ref} \cdot \frac{\partial\Delta\nu_i}{\partial TR_i^{ref}}\right)^2} \quad (54)$$

where ωTR_i was the uncertainty of the transmission ratio calculated at each pixel location in the data area for camera module i , and ωTR_i^{ref} was the uncertainty of the laser reference transmission ratio

for camera module i .¹⁰⁹ The partial derivatives in this equation were determined by calculating the partial derivatives of equation 53 with respect to the transmission ratio calculated at each pixel location in the data area for camera module i and the laser reference transmission ratio for camera module i . The values for these partial derivatives were calculated using the following equations:

Camera Module 1: (Above test section)

$$\frac{\partial \Delta v_1}{\partial TR_1} = c \cdot 100 \left(0.1855(TR_1)^4 - 0.2268(TR_1)^3 + 0.162(TR_1)^2 - 0.1002(TR_1) + 0.0364 \right) \quad (55)$$

$$\frac{\partial \Delta v_1}{\partial TR_1^{ref}} = -c \cdot 100 \left(0.1855(TR_1^{ref})^4 - 0.2268(TR_1^{ref})^3 + 0.162(TR_1^{ref})^2 - 0.1002(TR_1^{ref}) + 0.0364 \right) \quad (56)$$

Camera Module 2: (Port side of test section)

$$\frac{\partial \Delta v_2}{\partial TR_2} = c \cdot 100 \left(0.023(TR_2)^4 + 0.1796(TR_2)^3 - 0.2043(TR_2)^2 + 0.0390(TR_2) + 0.0018 \right) \quad (57)$$

$$\frac{\partial \Delta v_2}{\partial TR_2^{ref}} = -c \cdot 100 \left(0.023(TR_2^{ref})^4 + 0.1796(TR_2^{ref})^3 - 0.2043(TR_2^{ref})^2 + 0.0390(TR_2^{ref}) + 0.0018 \right) \quad (58)$$

Camera Module 3: (Starboard side of test section)

$$\frac{\partial \Delta v_3}{\partial TR_3} = c \cdot 100 \left(0.9445(TR_3)^4 - 1.9588(TR_3)^3 + 1.5198(TR_3)^2 - 0.5018(TR_3) + 0.0676 \right) \quad (59)$$

$$\frac{\partial \Delta v_3}{\partial TR_3^{ref}} = -c \cdot 100 \left(0.9445(TR_3^{ref})^4 - 1.9588(TR_3^{ref})^3 + 1.5198(TR_3^{ref})^2 - 0.5018(TR_3^{ref}) + 0.0676 \right) \quad (60)$$

where c was the speed of light.

7.1.1 Calculating Transmission Ratio Uncertainty

Before the uncertainty of the change in optical frequency ($\omega\Delta\nu_i$) could be calculated, the uncertainties ωTR_i and ωTR_i^{ref} needed to be calculated. The transmission ratio at a given pixel location (x, y) in the data area, $TR_i(x, y)$ was a function of the reference and filtered pixel intensities at that pixel location, so therefore, the uncertainty of the transmission ratio at pixel location (x, y) was calculated using the following equation:

$$\omega TR_i(x, y) = \sqrt{\left(\omega P_{filtered}(x, y) \cdot \frac{\partial TR_i(x, y)}{\partial P_{filtered}(x, y)}\right)^2 + \left(\omega P_{reference}(x, y) \cdot \frac{\partial TR_i(x, y)}{\partial P_{reference}(x, y)}\right)^2} \quad (61)$$

where $\omega P_{filtered}(x, y)$ was the uncertainty in the pixel intensity for the pixel in the filtered view at location (x, y) and $\omega P_{reference}(x, y)$ was the uncertainty in the pixel intensity for the pixel in the reference view at location (x, y) . The uncertainties in the filtered and reference view pixel intensities at location (x, y) were calculated using the standard deviation in the pixel intensities over the sequence of images reduced, the number of images within the sequence of images reduced, and Student's t distribution. The uncertainties in these pixel intensities were calculated using an equation of the following form:

$$\omega P = \frac{t\sigma}{\sqrt{n}} \quad (62)$$

where t was Student's t value, σ was the standard deviation in the mean pixel intensity, and n was the number of images in the sequence of images reduced.¹¹⁰ The values for the partial derivatives in equation 61 were calculated using the following equations:

$$\frac{\partial TR_i(x, y)}{\partial P_{filtered}(x, y)} = \frac{1}{P_{reference}(x, y)} \quad (63)$$

$$\frac{\partial TR_i(x, y)}{\partial P_{reference}(x, y)} = \frac{P_{filtered}(x, y)}{(P_{reference}(x, y))^2} \quad (64)$$

7.1.2 Calculating Laser Reference Transmission Ratio Uncertainty

A similar procedure was used to calculate the uncertainty in the calculated laser reference transmission ratio for each camera module. The following equation was used to calculate the laser reference transmission ratio for each camera module:

$$TR_i^{ref} = TR_{laser\ ROI} + \left(TR_{camera}^{ref} - TR_{laser\ ROI}^{ref} \right) \quad (65)$$

where TR_i^{ref} was the laser reference transmission ratio for camera module i , $TR_{laser\ ROI}$ was the average transmission ratio for the pixels inside the laser region of interest from the laser reference camera data image, TR_{camera}^{ref} was the average reference transmission ratio for camera module i , as described in subsection 4.5.5, and $TR_{laser\ ROI}^{ref}$ was the reference value of the laser reference transmission ratio from the laser reference camera, as described in section 4.5.3. From equation 65, the following equation was derived to calculate the uncertainty in the calculated value of the laser reference transmission ratio for camera module i :

$$\omega TR_i^{ref} = \sqrt{\left(\omega TR_{laser\ ROI} \cdot \frac{\partial TR_i^{ref}}{\partial TR_{laser\ ROI}} \right)^2 + \left(\omega TR_{laser\ ROI}^{ref} \cdot \frac{\partial TR_i^{ref}}{\partial TR_{laser\ ROI}^{ref}} \right)^2 + \left(\omega TR_{camera}^{ref} \cdot \frac{\partial TR_i^{ref}}{\partial TR_{camera}^{ref}} \right)^2} \quad (66)$$

The transmission ratio uncertainties, $\omega TR_{laser\ ROI}$, $\omega TR_{laser\ ROI}^{ref}$, and ωTR_{camera}^{ref} , were calculated using a series of equations of the form shown in equations 61 through 64. The standard deviations used to calculate $\omega TR_{laser\ ROI}$ and $\omega TR_{laser\ ROI}^{ref}$ were calculated from the filtered and reference pixel intensities for the pixels inside the laser reference regions of interest described in section 4.4.3. The standard deviations used to calculate ωTR_{camera}^{ref} were calculated from the filtered and reference pixel intensities for the pixels inside the filtered and reference regions of interest from the reference images acquired prior to acquiring velocity data from the calibration wheel. The values for the partial derivatives in equation 66 were calculated by taking the partial derivative of equation 65 with respect to $TR_{laser\ ROI}$, TR_{camera}^{ref} , and $TR_{laser\ ROI}^{ref}$. The partial derivative of the laser reference transmission ratio for camera module i , with respect to the average transmission ratio for the pixels inside the laser region

of interest from the laser reference camera data image, TR_{ROI}^{laser} , was 1. The partial derivative of the laser reference transmission ratio for camera module i , with respect to the reference value of the laser reference transmission ratio from the laser reference camera, TR_{ROI}^{ref} , was -1. The partial derivative of the laser reference transmission ratio for camera module i , with respect to the average reference transmission ratio from camera module i , TR_{camera}^{ref} , was 1. Once the uncertainty of the transmission ratio at each pixel location in the data area and the uncertainty of the laser reference transmission ratio had been calculated for camera module i , equation 54 could be used to solve for the uncertainty of the change in optical frequency measured by camera module i , $\omega\Delta v_i$, could be calculated.

7.1.3 Calculating Velocity Partial Derivatives with respect to Δv

The governing equation for the DGV technique shown in equation 51 can also be expressed in the following manner:

$$V_x = m_{11}\Delta v_1 + m_{12}\Delta v_2 + m_{13}\Delta v_3 \quad (67)$$

$$V_y = m_{21}\Delta v_1 + m_{22}\Delta v_2 + m_{23}\Delta v_3 \quad (68)$$

$$V_z = m_{31}\Delta v_1 + m_{32}\Delta v_2 + m_{33}\Delta v_3 \quad (69)$$

where

$$m_{11} = \lambda \cdot a_{11} \quad (70)$$

$$m_{12} = \lambda \cdot a_{12} \quad (71)$$

$$m_{13} = \lambda \cdot a_{13} \quad \text{and so on....} \quad (72)$$

The $a_{i,j}$ terms in equations 70-72 correspond to the terms in the inverse matrix shown in equation 51 and the λ term is the wavelength of the laser pulse which is equal to the reciprocal of the wave number. Taking the partial derivatives of each velocity component with respect to Δv_i gives the following results:

$$\frac{\partial V_x}{\partial \Delta v_1} = m_{11} = \lambda \cdot a_{11} \quad (73)$$

$$\frac{\partial V_x}{\partial \Delta v_2} = m_{12} = \lambda \cdot a_{12} \quad (74)$$

$$\frac{\partial V_x}{\partial \Delta \nu_3} = m_{13} = \lambda \cdot a_{13} \quad (75)$$

$$\frac{\partial V_y}{\partial \Delta \nu_1} = m_{21} = \lambda \cdot a_{21} \quad (76)$$

$$\frac{\partial V_y}{\partial \Delta \nu_2} = m_{22} = \lambda \cdot a_{22} \quad \text{and so on....} \quad (77)$$

Using the Euler angles calculated for each of the camera modules and the laser propagation vector calculated in Chapter 6 the values for the partial derivatives of each velocity component with respect to the change in optical frequency measured by each camera module were:

$$\begin{bmatrix} \frac{\partial V_x}{\partial \Delta \nu_1} & \frac{\partial V_x}{\partial \Delta \nu_2} & \frac{\partial V_x}{\partial \Delta \nu_3} \\ \frac{\partial V_y}{\partial \Delta \nu_1} & \frac{\partial V_y}{\partial \Delta \nu_2} & \frac{\partial V_y}{\partial \Delta \nu_3} \\ \frac{\partial V_z}{\partial \Delta \nu_1} & \frac{\partial V_z}{\partial \Delta \nu_2} & \frac{\partial V_z}{\partial \Delta \nu_3} \end{bmatrix} = \frac{1}{WN} \begin{bmatrix} 0.391437 & -1.47640 & 1.08858 \\ -1.92423 & 0.813357 & 1.03147 \\ 0.0626446 & -0.662552 & 0.0382006 \end{bmatrix} \quad (78)$$

where WN was the wave number of the pulse used to acquire velocity data.

7.2 Calculating Wave Number Uncertainty

The procedure used to calculate the uncertainty for the wave number used some of the same information used to calculate the uncertainty for the change in optical frequency, so this procedure will be discussed next. As was discussed in Chapter 2, the wave number is defined as 1/wavelength. The frequency calibration functions given in equations 47 – 49 were used to calculate the wave number for the laser pulse as well as calculating the optical frequency at each pixel location in the data area. A wave number was calculated using laser reference transmission ratio from each camera module, TR_i^{ref} . The three wave numbers were then averaged to calculate an average wave number, which was used in the data reduction procedure. Because the laser reference transmission ratio from each camera module was used in calculating the wave number used in the data reduction procedure, the equation used to calculate the uncertainty of the calculated wave number was:

$$\omega WN = \sqrt{\left(\omega TR_1^{ref} \cdot \frac{\partial WN}{\partial TR_1^{ref}}\right)^2 + \left(\omega TR_2^{ref} \cdot \frac{\partial WN}{\partial TR_2^{ref}}\right)^2 + \left(\omega TR_3^{ref} \cdot \frac{\partial WN}{\partial TR_3^{ref}}\right)^2} \quad (79)$$

where ωWN was the uncertainty of the wave number, and ωTR_1^{ref} , ωTR_2^{ref} , and ωTR_3^{ref} were the uncertainties in the laser reference transmission ratios for camera modules 1, 2, and 3 respectively. The uncertainties ωTR_1^{ref} , ωTR_2^{ref} , and ωTR_3^{ref} were calculated as part of the procedure used to calculate the uncertainty of the changes in optical frequency, $\Delta \nu_1$, $\Delta \nu_2$, and $\Delta \nu_3$, (see section 7.1.2). All that was needed was to calculate the partial derivatives in equation 79. The equations used to calculate the values for these partial derivatives are given below.

Camera Module 1: (Above test section)

$$\frac{\partial WN}{\partial TR_1^{ref}} = 100 \left(0.1855 (TR_1^{ref})^4 - 0.2268 (TR_1^{ref})^3 + 0.162 (TR_1^{ref})^2 - 0.1002 (TR_1^{ref}) + 0.0364 \right) \quad (80)$$

Camera Module 2: (Port side of test section)

$$\frac{\partial WN}{\partial TR_2} = 100 \left(0.023 (TR_2^{ref})^4 + 0.1796 (TR_2^{ref})^3 - 0.2043 (TR_2^{ref})^2 + 0.0390 (TR_2^{ref}) + 0.0018 \right) \quad (81)$$

Camera Module 3: (Starboard side of test section)

$$\frac{\partial WN}{\partial TR_3} = 100 \left(0.9445 (TR_3^{ref})^4 - 1.9588 (TR_3^{ref})^3 + 1.5198 (TR_3^{ref})^2 - 0.5018 (TR_3^{ref}) + 0.0676 \right) \quad (82)$$

The partial derivative of velocity with respect to wave number, found in equation 52, was calculated to be:

$$\begin{pmatrix} \frac{\partial V_x}{\partial WN} \\ \frac{\partial V_y}{\partial WN} \\ \frac{\partial V_z}{\partial WN} \end{pmatrix} = \frac{1}{WN^2} \begin{bmatrix} \sin \theta_{y1} + \sin \theta_{ylas} & -\sin \theta_{x1} \cos \theta_{y1} - \sin \theta_{xlas} \cos \theta_{ylas} & -\cos \theta_{x1} \cos \theta_{y1} - \cos \theta_{xlas} \cos \theta_{ylas} \\ \sin \theta_{y2} + \sin \theta_{ylas} & -\sin \theta_{x2} \cos \theta_{y2} - \sin \theta_{xlas} \cos \theta_{ylas} & -\cos \theta_{x2} \cos \theta_{y2} - \cos \theta_{xlas} \cos \theta_{ylas} \\ \sin \theta_{x3} + \sin \theta_{ylas} & -\sin \theta_{x3} \cos \theta_{y3} - \sin \theta_{xlas} \cos \theta_{ylas} & -\cos \theta_{x3} \cos \theta_{y3} - \cos \theta_{xlas} \cos \theta_{ylas} \end{bmatrix}^{-1} \begin{pmatrix} \Delta \nu_1 \\ \Delta \nu_2 \\ \Delta \nu_3 \end{pmatrix} \quad (83)$$

Inserting the Euler angles for the camera module viewing angles and the laser propagation vector calculated in Chapter 6, equation 83 becomes:

$$\begin{Bmatrix} \frac{\partial V_x}{\partial WN} \\ \frac{\partial V_y}{\partial WN} \\ \frac{\partial V_z}{\partial WN} \end{Bmatrix} = \frac{1}{WN^2} \begin{bmatrix} 0.391437 & -1.47640 & 1.08858 \\ -1.92423 & 0.813357 & 1.03147 \\ 0.0626446 & -0.662552 & 0.0382006 \end{bmatrix} \cdot \begin{Bmatrix} \Delta v_1 \\ \Delta v_2 \\ \Delta v_3 \end{Bmatrix} \quad (84)$$

7.3 Calculating Angle Uncertainties

7.3.1 Viewing angle uncertainty

As was discussed in the M. S thesis of Troy Jones, the camera calibration toolbox used to calculate the Euler angles for each of the camera modules did not provide direct uncertainties on the extrinsic properties output by the toolbox.¹¹¹ The toolbox did output average pixel errors but these values were a measure of the accuracy of the analytical reprojection of the reference points input into the toolbox and not an indicator of the accuracy of the rotation matrix output by the program. Jones performed an iterative procedure where small perturbations to the Euler angles calculated by the toolbox were made and the change in the observation vector was calculated. From this analysis, Jones estimated the uncertainties for all of these angles to be $\pm 0.75^\circ$, or ± 0.013090 radians.¹¹² This uncertainty value was also used in the current uncertainty analysis.

7.3.2 Laser Propagation Vector Uncertainty

Because the laser propagation vector used to reduce the calibration wheel data was calculated from estimated Euler angles, the uncertainties for these angles are considerably higher than those calculated for the camera Euler angles. The uncertainties for the $\theta_{x\text{las}}$ and $\theta_{y\text{las}}$ angles used to calculate the laser propagation vector were both assumed to be $\pm 3^\circ$, or ± 0.052360 radians.

7.3.3 Partial Derivatives for the Angular Measurements

The partial derivatives of each of the velocity components with respect to each of the angular measurements used in reducing the calibration wheel data were calculated using Mathematica. Mathematica was chosen to perform these calculations because these partial derivatives were too complicated to calculate by hand and Mathematica had the ability to perform mathematical operations on symbolic expressions. The following equations were obtained from Mathematica and used in this uncertainty analysis:

$$\begin{Bmatrix} \frac{\partial V_x}{\partial \theta_{x1}} \\ \frac{\partial V_y}{\partial \theta_{x1}} \\ \frac{\partial V_z}{\partial \theta_{x1}} \end{Bmatrix} = \lambda \begin{bmatrix} -0.650550 & 0.407580 & 0.333758 \\ 3.19799 & -2.00359 & -1.64070 \\ -0.104113 & 0.0652282 & 0.0534139 \end{bmatrix} \begin{Bmatrix} \Delta f_1 \\ \Delta f_2 \\ \Delta f_3 \end{Bmatrix} \quad (100)$$

$$\begin{Bmatrix} \frac{\partial V_x}{\partial \theta_{x2}} \\ \frac{\partial V_y}{\partial \theta_{x2}} \\ \frac{\partial V_z}{\partial \theta_{x2}} \end{Bmatrix} = \lambda \begin{bmatrix} 2.59546 & -1.18932 & -1.38087 \\ -1.42986 & 0.655203 & 0.760728 \\ 1.16475 & -0.533721 & -0.619681 \end{bmatrix} \begin{Bmatrix} \Delta f_1 \\ \Delta f_2 \\ \Delta f_3 \end{Bmatrix} \quad (101)$$

$$\begin{Bmatrix} \frac{\partial V_x}{\partial \theta_{x3}} \\ \frac{\partial V_y}{\partial \theta_{x3}} \\ \frac{\partial V_z}{\partial \theta_{x3}} \end{Bmatrix} = \lambda \begin{bmatrix} -1.93891 & 0.779342 & 1.04388 \\ -1.83719 & 0.738456 & 0.989113 \\ -0.0680407 & 0.0273488 & 0.0366319 \end{bmatrix} \begin{Bmatrix} \Delta f_1 \\ \Delta f_2 \\ \Delta f_3 \end{Bmatrix} \quad (102)$$

$$\begin{Bmatrix} \frac{\partial V_x}{\partial \theta_{y1}} \\ \frac{\partial V_y}{\partial \theta_{y1}} \\ \frac{\partial V_z}{\partial \theta_{y1}} \end{Bmatrix} = \lambda \begin{bmatrix} -0.150405 & 0.578270 & -0.427782 \\ 0.739364 & -2.84267 & 2.10290 \\ -0.0240704 & 0.0925450 & -0.0684613 \end{bmatrix} \begin{Bmatrix} \Delta f_1 \\ \Delta f_2 \\ \Delta f_3 \end{Bmatrix} \quad (103)$$

$$\begin{Bmatrix} \frac{\partial V_x}{\partial \theta_{y2}} \\ \frac{\partial V_y}{\partial \theta_{y2}} \\ \frac{\partial V_z}{\partial \theta_{y2}} \end{Bmatrix} = \lambda \begin{bmatrix} 0.614704 & -1.65685 & 1.38347 \\ -0.338644 & 0.912769 & -0.762163 \\ 0.275856 & -0.743531 & 0.620849 \end{bmatrix} \begin{Bmatrix} \Delta f_1 \\ \Delta f_2 \\ \Delta f_3 \end{Bmatrix} \quad (104)$$

$$\begin{pmatrix} \frac{\partial V_x}{\partial \theta_{y3}} \\ \frac{\partial V_y}{\partial \theta_{y3}} \\ \frac{\partial V_z}{\partial \theta_{y3}} \end{pmatrix} = \lambda \begin{bmatrix} -0.469470 & 1.77982 & -1.09069 \\ -0.444841 & 1.68645 & -1.03347 \\ -0.0164747 & 0.0624579 & -0.0382747 \end{bmatrix} \begin{pmatrix} \Delta f_1 \\ \Delta f_2 \\ \Delta f_3 \end{pmatrix} \quad (105)$$

$$\begin{pmatrix} \frac{\partial V_x}{\partial \theta_{xlas}} \\ \frac{\partial V_y}{\partial \theta_{xlas}} \\ \frac{\partial V_z}{\partial \theta_{xlas}} \end{pmatrix} = \lambda \begin{bmatrix} -0.00599899 & 0.00239674 & 0.00323139 \\ 0.131703 & -0.0526185 & -0.0709426 \\ 0.931642 & -0.372213 & -0.501835 \end{bmatrix} \begin{pmatrix} \Delta f_1 \\ \Delta f_2 \\ \Delta f_3 \end{pmatrix} \quad (106)$$

$$\begin{pmatrix} \frac{\partial V_x}{\partial \theta_{ylas}} \\ \frac{\partial V_y}{\partial \theta_{ylas}} \\ \frac{\partial V_z}{\partial \theta_{ylas}} \end{pmatrix} = \lambda \begin{bmatrix} -0.00158187 & 0.00592247 & -0.0033486 \\ 0.0347288 & -0.130023 & 0.0735158 \\ 0.245665 & -0.919759 & 0.520036 \end{bmatrix} \begin{pmatrix} \Delta f_1 \\ \Delta f_2 \\ \Delta f_3 \end{pmatrix} \quad (107)$$

where λ was the wavelength, which was equal to 1/wave number. These were the last terms needed to solve equation 52 for the uncertainty of each velocity component. This procedure was different from the one used by Troy Jones to calculate these partial derivatives. He calculated these partial derivatives using a perturbation technique similar to the one he used to calculate the uncertainties in the camera Euler angles.¹¹³

7.4 Uncertainty Analysis Results

Figures 7.1, 7.2, and 7.3 are contour plots of the uncertainties for the velocity components in the x, y, and z directions, respectively. Figure 7.1 shows that the uncertainties for the velocity components in the x direction vary from roughly 9 m/s to 28 m/s. Figure 7.2 shows that the uncertainties for the velocity components in the y direction vary from roughly 20 m/s to 55 m/s. Figure 7.3 shows that the uncertainties for the velocity components in the z direction vary from roughly 1.5 m/s to 11.75 m/s. Given the results shown in Chapter 6, the large uncertainties shown

here were to be expected. More will be said about the primary sources of the large uncertainties shown here later in this chapter.

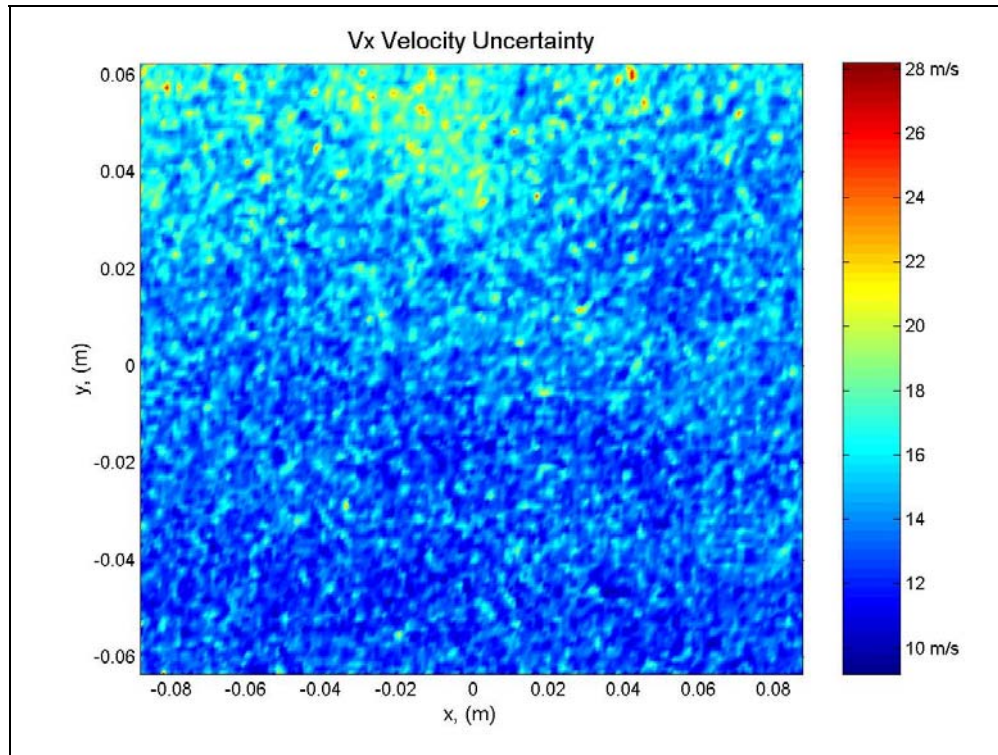


Figure 7.1: Uncertainty of the velocity components in the x direction.

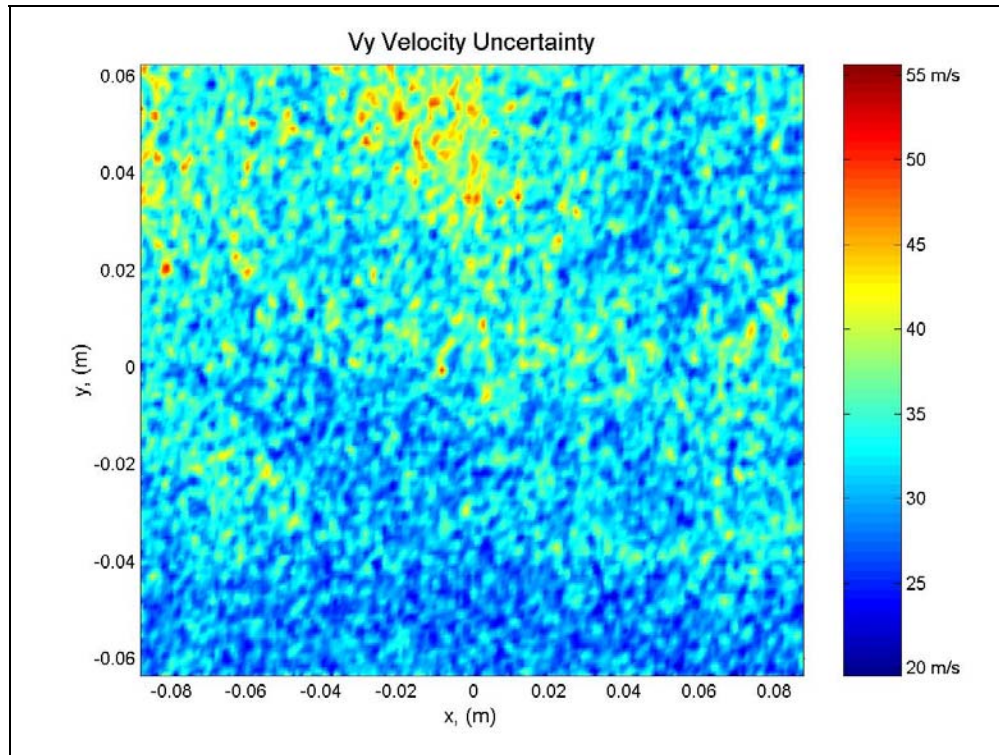


Figure 7.2: Uncertainty of the velocity components in the y direction.

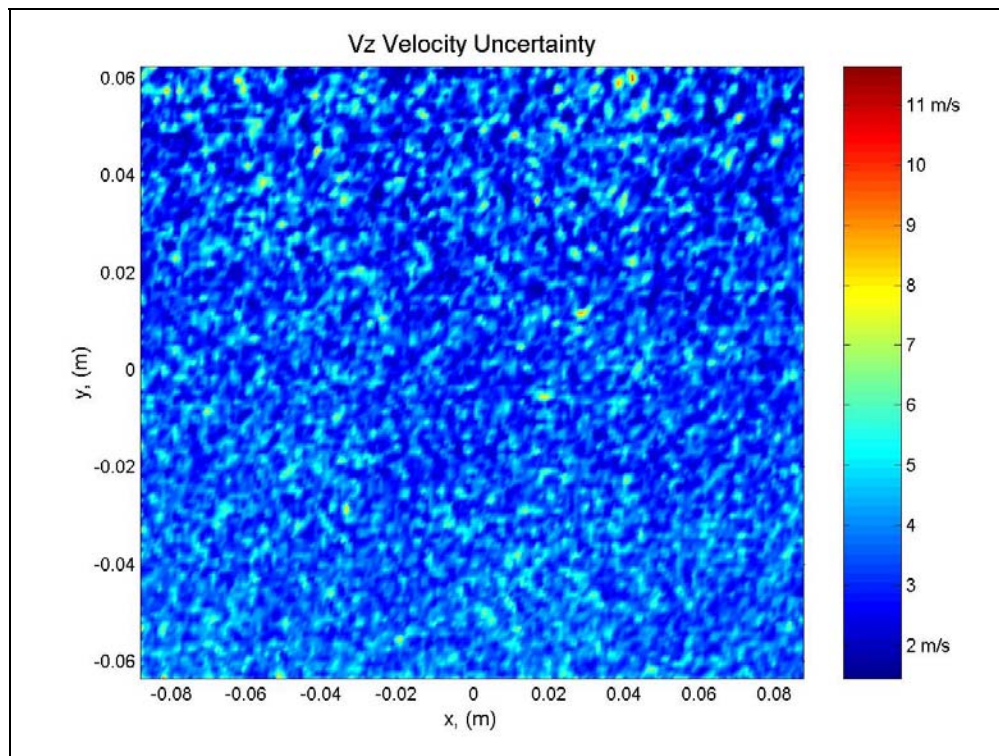


Figure 7.3: Uncertainty of the velocity components in the z direction.

Figures 7.4 and 7.5 show the upper and lower bounds for the V_x velocity uncertainties applied to plots of the V_x velocity component measured along the vertical and horizontal centerlines of the calibration wheel. Figures 7.6 and 7.7 show the upper and lower bounds for the V_y velocity uncertainties applied to plots of the V_y velocity component along the vertical and horizontal centerlines of the calibration wheel. Figures 7.8 and 7.9 show the upper and lower bounds for the V_z velocity uncertainties applied to plots of the V_z velocity along the vertical and horizontal centerlines of the calibration wheel.

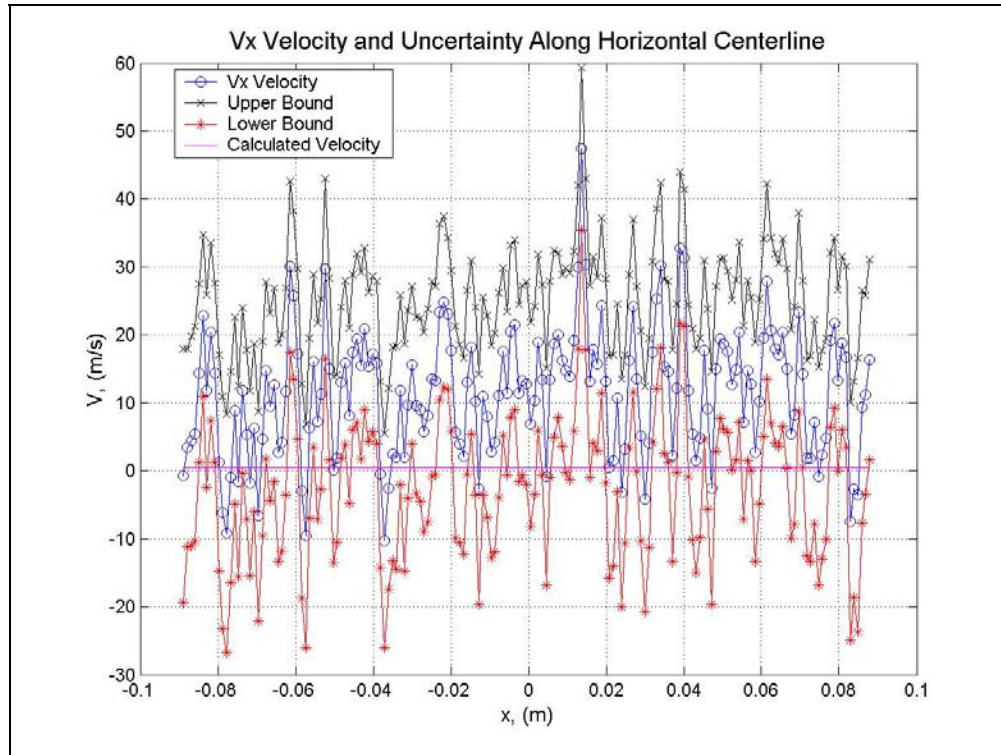


Figure 7.4: Upper and lower bounds on V_x velocity uncertainty and V_x velocity component along horizontal centerline of calibration wheel.

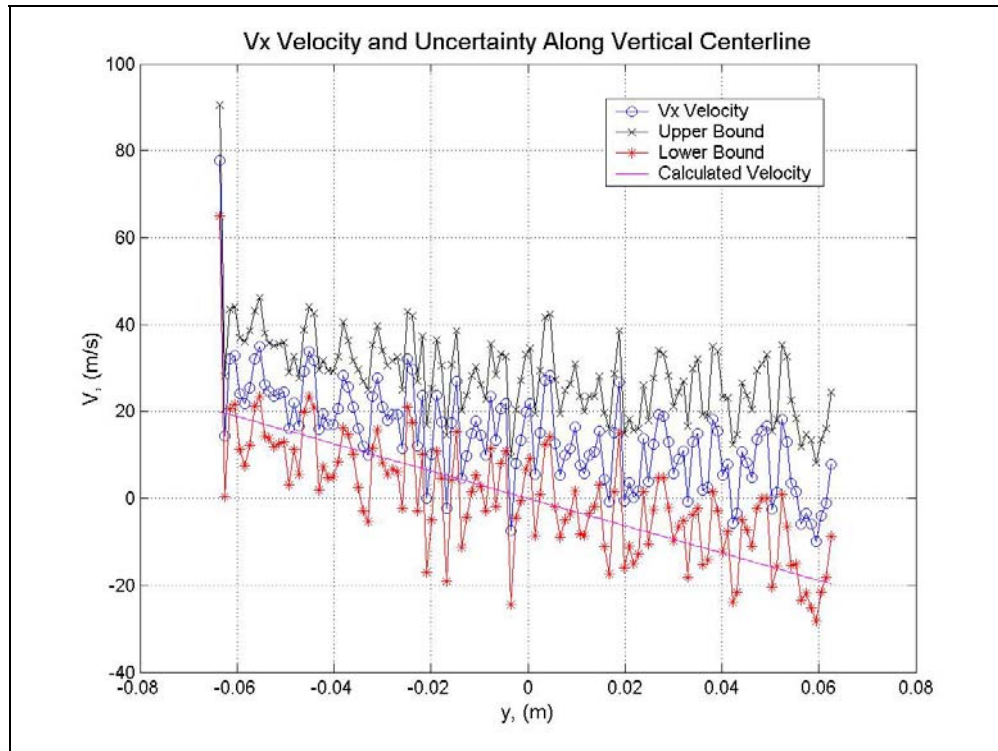


Figure 7.5: Upper and lower bounds on V_x velocity uncertainty and V_x velocity component along vertical centerline of calibration wheel.

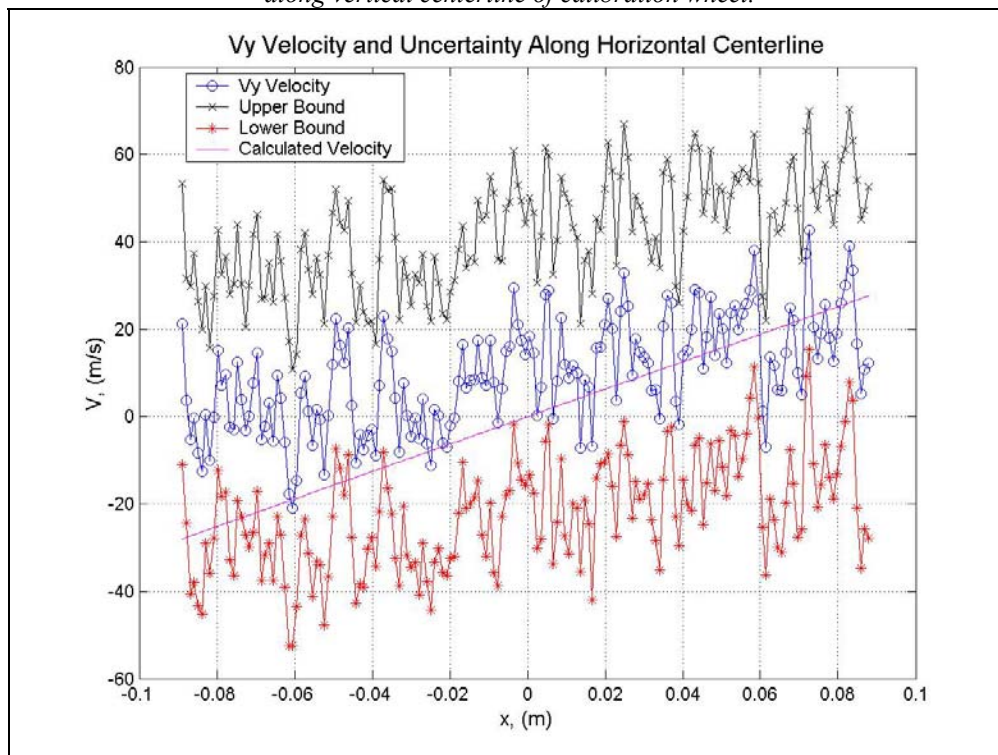


Figure 7.6: Upper and lower bounds on V_y velocity uncertainty and V_y velocity component along horizontal centerline of calibration wheel.

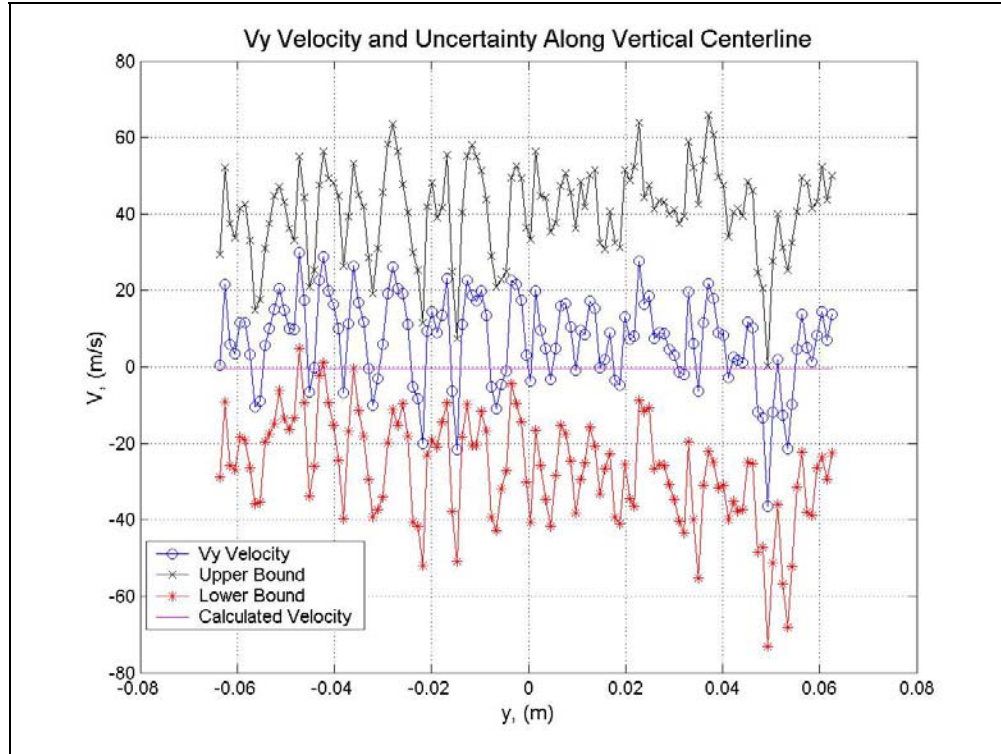


Figure 7.7: Upper and lower bounds on V_y velocity uncertainty and V_y velocity component along vertical centerline of calibration wheel.

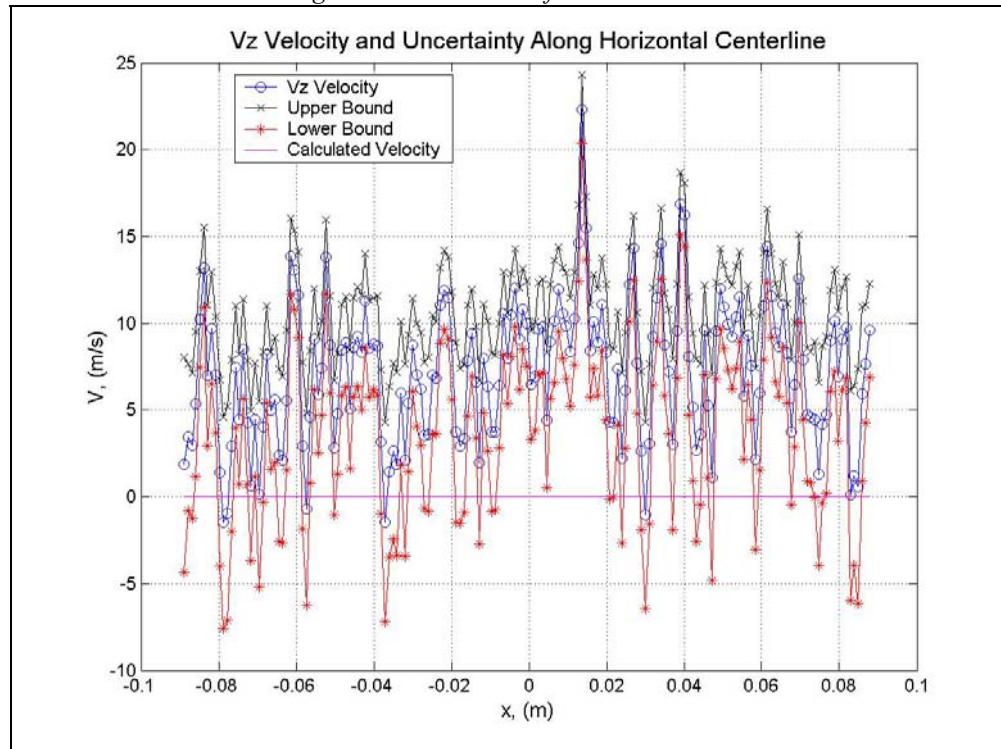


Figure 7.8: Upper and lower bounds on V_z velocity uncertainty and V_z velocity component along horizontal centerline of calibration wheel.

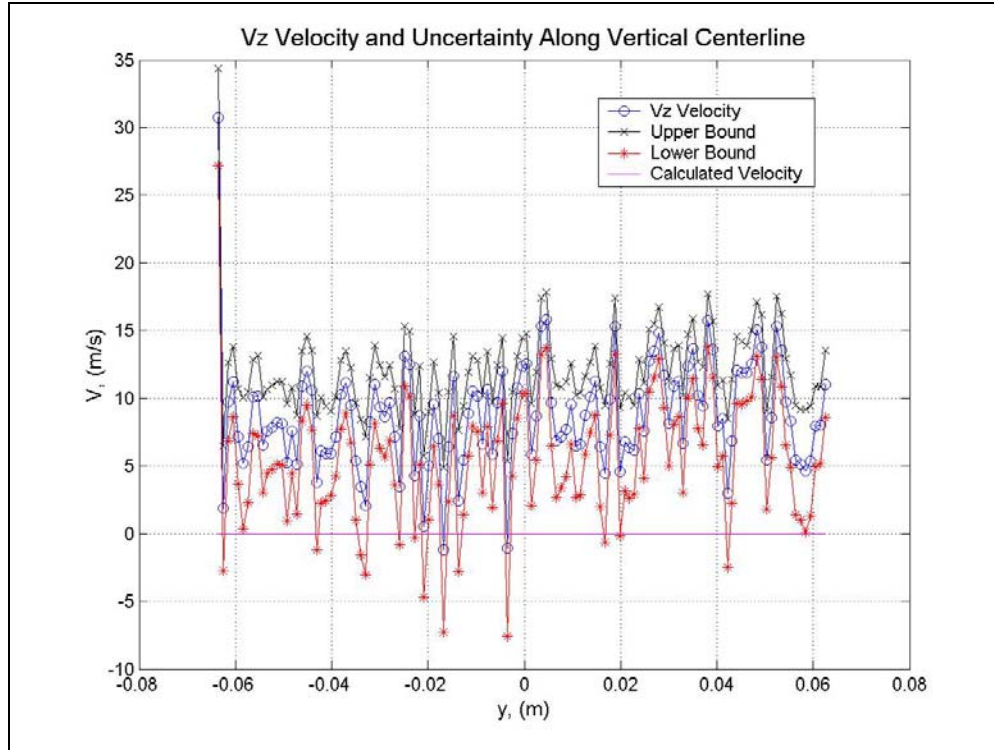


Figure 7.9: Upper and lower bounds on V_z velocity uncertainty and V_z velocity component along vertical centerline of calibration wheel.

7.5 Analysis of Uncertainty Components

An analysis of the calculated values for each term in equation 52 will reveal the largest sources of uncertainty in the measured calibration wheel velocities. Determining the largest sources of uncertainty will provide direction for where improvements can and should be made to the VT DGV system in the future. The average uncertainty for each velocity component will be calculated as part of this analysis.

7.5.1 Optical Frequency Uncertainty

The first step in calculating the average uncertainty of the measured change in optical frequency was to calculate the uncertainties in the transmission ratios TR_i and TR_i^{ref} , as was discussed in sections 7.1.1 and 7.1.2. The average uncertainty values calculated for the transmission ratios in the data area were: $\omega TR_1 = 0.08227$, $\omega TR_2 = 0.09755$, and $\omega TR_3 = 0.04229$. The average uncertainty values calculated for the laser reference transmission ratio from each camera module were: $\omega TR_1^{ref} = 0.01253$, $\omega TR_2^{ref} = 0.01255$, and $\omega TR_3^{ref} = 0.01251$. Next, the partial derivatives of the change in optical frequency with respect to the data area transmission ratios and laser reference

transmission ratios were calculated. The average values calculated for the partial derivatives of the change in optical frequency with respect to the data area transmission ratios were:

$$\frac{\partial \Delta \nu_1}{\partial TR_1} = 3.6511 \times 10^8 \quad (108)$$

$$\frac{\partial \Delta \nu_2}{\partial TR_2} = -9.5744 \times 10^7 \quad (109)$$

$$\frac{\partial \Delta \nu_3}{\partial TR_3} = 3.9646 \times 10^8 \quad (110)$$

The average values calculated for the partial derivatives of the change in optical frequency with respect to the laser reference transmission ratios for each camera module were:

$$\frac{\partial \Delta \nu_1}{\partial TR_1^{ref}} = 3.1925 \times 10^8 \quad (111)$$

$$\frac{\partial \Delta \nu_2}{\partial TR_2^{ref}} = -1.4999 \times 10^8 \quad (112)$$

$$\frac{\partial \Delta \nu_3}{\partial TR_3^{ref}} = 3.8415 \times 10^8 \quad (113)$$

Once the uncertainties for the data area and laser reference transmission ratios and the partial derivatives of the change in optical frequency with respect to the data area and laser reference transmission ratios had been calculated, the uncertainty in the measured change in optical frequency was calculated using equation 54. The following average uncertainty values were obtained:

$$\omega \Delta \nu_1 = 3.0304 \times 10^7, \quad \omega \Delta \nu_2 = 9.5273 \times 10^6, \quad \text{and} \quad \omega \Delta \nu_3 = 1.7442 \times 10^7.$$

Next, the partial derivatives of each velocity component with respect to the change in optical frequency measured by each camera module were calculated. The following average values for these partial derivatives were obtained:

$$\begin{bmatrix} \frac{\partial V_x}{\partial \Delta \nu_1} & \frac{\partial V_x}{\partial \Delta \nu_2} & \frac{\partial V_x}{\partial \Delta \nu_3} \\ \frac{\partial V_y}{\partial \Delta \nu_1} & \frac{\partial V_y}{\partial \Delta \nu_2} & \frac{\partial V_y}{\partial \Delta \nu_3} \\ \frac{\partial V_z}{\partial \Delta \nu_1} & \frac{\partial V_z}{\partial \Delta \nu_2} & \frac{\partial V_z}{\partial \Delta \nu_3} \end{bmatrix} = (1 \times 10^{-7}) \begin{bmatrix} 2.0835 & -7.8582 & 5.7940 \\ -10.241 & 4.3291 & 1.03147 \\ 0.33343 & -3.5265 & 0.20332 \end{bmatrix} \quad (114)$$

Once the average uncertainties in the measured change in optical frequency for each camera module and average values for the partial derivatives of each velocity component with respect to the change in optical frequency measured by each camera module had been calculated, the terms input into equation 52 were calculated. The values for these terms were as follows:

$$\left(\omega \Delta \nu_1 \cdot \frac{\partial V_x}{\partial \Delta \nu_1} \right)^2 = 39.865 \quad (115)$$

$$\left(\omega \Delta \nu_2 \cdot \frac{\partial V_x}{\partial \Delta \nu_2} \right)^2 = 56.051 \quad (116)$$

$$\left(\omega \Delta \nu_3 \cdot \frac{\partial V_x}{\partial \Delta \nu_3} \right)^2 = 102.129 \quad (117)$$

$$\left(\omega \Delta \nu_1 \cdot \frac{\partial V_y}{\partial \Delta \nu_1} \right)^2 = 963.129 \quad (118)$$

$$\left(\omega \Delta \nu_2 \cdot \frac{\partial V_y}{\partial \Delta \nu_2} \right)^2 = 17.011 \quad (119)$$

$$\left(\omega \Delta \nu_3 \cdot \frac{\partial V_y}{\partial \Delta \nu_3} \right)^2 = 3.237 \quad (120)$$

$$\left(\omega \Delta \nu_1 \cdot \frac{\partial V_z}{\partial \Delta \nu_1} \right)^2 = 1.021 \quad (121)$$

$$\left(\omega \Delta \nu_2 \cdot \frac{\partial V_z}{\partial \Delta \nu_2} \right)^2 = 11.288 \quad (122)$$

$$\left(\omega \Delta \nu_3 \cdot \frac{\partial V_z}{\partial \Delta \nu_3} \right)^2 = 0.125 \quad (123)$$

7.5.2 Wave Number Uncertainty

Next, the wave number uncertainty was calculated using equation 79. As was discussed in section 7.2, the uncertainties of the laser reference transmission ratio for each camera module, ωTR_1^{ref} , ωTR_2^{ref} , and ωTR_3^{ref} , were calculated as part of the procedure used to calculate the uncertainty of the changes in optical frequency $\Delta \nu_1$, $\Delta \nu_2$, and $\Delta \nu_3$. The partial derivatives of wave number with respect to TR_1^{ref} , TR_2^{ref} , and TR_3^{ref} were calculated using equations 80-82. The following values were obtained for these partial derivatives:

$$\frac{\partial WN}{\partial TR_1^{ref}} = 1.0649 \quad (124)$$

$$\frac{\partial WN}{\partial TR_2^{ref}} = -0.5000 \quad (125)$$

$$\frac{\partial WN}{\partial TR_3^{ref}} = 1.2814 \quad (126)$$

The uncertainties of the laser reference transmission ratios for each of the camera modules and the values for the partial derivatives shown in equations 124 through 126 were used to calculate the uncertainty of the wave number. The value calculated for the uncertainty of the wave number was $\omega WN = 2.1779 \times 10^{-2}$.

After the uncertainty of the wave number had been calculated, the partial derivative of each velocity component with respect to the wave number was calculated using equation 84. The calculated values for these partial derivatives were as follows:

$$\frac{\partial V_x}{\partial WN} = 5.9426 \times 10^{-6} \quad (127)$$

$$\frac{\partial V_y}{\partial WN} = 4.8131 \times 10^{-6} \quad (128)$$

$$\frac{\partial V_z}{\partial \omega WN} = 5.7329 \times 10^{-6} \quad (129)$$

Once the uncertainty of the wave number and the partial derivative of each velocity component with respect to the wave number had been calculated, the wave number term in equation 52 was calculated for each velocity component. The calculated values for these terms were:

$$\left(\omega WN \cdot \frac{\partial V_x}{\partial \omega WN} \right)^2 = 1.6751 \times 10^{-14} \quad (130)$$

$$\left(\omega WN \cdot \frac{\partial V_y}{\partial \omega WN} \right)^2 = 1.0988 \times 10^{-14} \quad (131)$$

$$\left(\omega WN \cdot \frac{\partial V_z}{\partial \omega WN} \right)^2 = 1.5589 \times 10^{-14} \quad (132)$$

7.5.3 Angular Measurement Uncertainty

The uncertainties in the Euler angles for each camera module and for the Euler angles used to calculate the laser propagation vector were given in sections 7.3.1 and 7.3.2 respectively. All that is needed is to calculate the partial derivatives for the velocity components with respect to each of these Euler angles. The average values calculated for the partial derivatives of each velocity component with respect to the θ_x Euler angles for the camera modules were:

$$\begin{bmatrix} \frac{\partial V_x}{\partial \theta_{x1}} & \frac{\partial V_x}{\partial \theta_{x2}} & \frac{\partial V_x}{\partial \theta_{x3}} \\ \frac{\partial V_y}{\partial \theta_{x1}} & \frac{\partial V_y}{\partial \theta_{x2}} & \frac{\partial V_y}{\partial \theta_{x3}} \\ \frac{\partial V_z}{\partial \theta_{x1}} & \frac{\partial V_z}{\partial \theta_{x2}} & \frac{\partial V_z}{\partial \theta_{x3}} \end{bmatrix} = \begin{bmatrix} 0.7505 & -10.593 & 9.811 \\ -3.698 & 5.836 & 9.297 \\ 0.1201 & -4.754 & 0.3443 \end{bmatrix} \quad (133)$$

The average values calculated for the partial derivatives of each velocity component with respect to the θ_j Euler angles for the camera modules were:

$$\begin{bmatrix} \frac{\partial V_x}{\partial \theta_{y1}} & \frac{\partial V_x}{\partial \theta_{y2}} & \frac{\partial V_x}{\partial \theta_{y3}} \\ \frac{\partial V_y}{\partial \theta_{y1}} & \frac{\partial V_y}{\partial \theta_{y2}} & \frac{\partial V_y}{\partial \theta_{y3}} \\ \frac{\partial V_z}{\partial \theta_{y1}} & \frac{\partial V_z}{\partial \theta_{y2}} & \frac{\partial V_z}{\partial \theta_{y3}} \end{bmatrix} = \begin{bmatrix} -4.411 & 8.164 & -15.389 \\ 21.682 & -4.498 & -14.581 \\ -0.7059 & 3.664 & -0.5400 \end{bmatrix} \quad (134)$$

The average values calculated for the partial derivatives of each velocity component with respect to the Euler angles used to calculate the laser propagation vector were:

$$\begin{bmatrix} \frac{\partial V_x}{\partial \theta_{xlas}} & \frac{\partial V_x}{\partial \theta_{ylas}} \\ \frac{\partial V_y}{\partial \theta_{xlas}} & \frac{\partial V_y}{\partial \theta_{ylas}} \\ \frac{\partial V_z}{\partial \theta_{xlas}} & \frac{\partial V_z}{\partial \theta_{ylas}} \end{bmatrix} = \begin{bmatrix} 0.03061 & -0.05326 \\ -0.6720 & 1.169 \\ -4.754 & 8.272 \end{bmatrix} \quad (135)$$

Once the values for all of the partial derivatives were calculated, the angular measurement uncertainty terms in equation 52 were calculated. The average values calculated for the uncertainty terms containing the θ_x Euler angle for each of the camera modules were:

$$\begin{bmatrix} \left(\omega \theta_{x1} \cdot \frac{\partial V_x}{\partial \theta_{x1}} \right)^2 & \left(\omega \theta_{x2} \cdot \frac{\partial V_x}{\partial \theta_{x2}} \right)^2 & \left(\omega \theta_{x3} \cdot \frac{\partial V_x}{\partial \theta_{x3}} \right)^2 \\ \left(\omega \theta_{x1} \cdot \frac{\partial V_y}{\partial \theta_{x1}} \right)^2 & \left(\omega \theta_{x2} \cdot \frac{\partial V_y}{\partial \theta_{x2}} \right)^2 & \left(\omega \theta_{x3} \cdot \frac{\partial V_y}{\partial \theta_{x3}} \right)^2 \\ \left(\omega \theta_{x1} \cdot \frac{\partial V_z}{\partial \theta_{x1}} \right)^2 & \left(\omega \theta_{x2} \cdot \frac{\partial V_z}{\partial \theta_{x2}} \right)^2 & \left(\omega \theta_{x3} \cdot \frac{\partial V_z}{\partial \theta_{x3}} \right)^2 \end{bmatrix} = (1 \times 10^{-2}) \begin{bmatrix} 0.009651 & 1.9227 & 1.6493 \\ 0.2343 & 0.5836 & 1.4810 \\ 0.000247 & 0.3873 & 0.002031 \end{bmatrix} \quad (136)$$

The average values calculated for the uncertainty terms containing the θ , Euler angle for each of the camera modules were:

$$\begin{bmatrix} \left(\omega\theta_{y1} \cdot \frac{\partial V_x}{\partial \theta_{y1}} \right)^2 & \left(\omega\theta_{y2} \cdot \frac{\partial V_x}{\partial \theta_{y2}} \right)^2 & \left(\omega\theta_{y3} \cdot \frac{\partial V_x}{\partial \theta_{y3}} \right)^2 \\ \left(\omega\theta_{y1} \cdot \frac{\partial V_y}{\partial \theta_{y1}} \right)^2 & \left(\omega\theta_{y2} \cdot \frac{\partial V_y}{\partial \theta_{y2}} \right)^2 & \left(\omega\theta_{y3} \cdot \frac{\partial V_y}{\partial \theta_{y3}} \right)^2 \\ \left(\omega\theta_{y1} \cdot \frac{\partial V_z}{\partial \theta_{y1}} \right)^2 & \left(\omega\theta_{y2} \cdot \frac{\partial V_z}{\partial \theta_{y2}} \right)^2 & \left(\omega\theta_{y3} \cdot \frac{\partial V_z}{\partial \theta_{y3}} \right)^2 \end{bmatrix} = (1 \times 10^{-2}) \begin{bmatrix} 0.3334 & 1.1420 & 4.0579 \\ 8.0552 & 0.3467 & 3.6429 \\ 0.008538 & 0.2300 & 0.004996 \end{bmatrix} \quad (137)$$

The average values calculated for the uncertainty terms containing the θ_{xlas} and θ_{ylas} Euler angles used to calculate the laser propagation vector were:

$$\begin{bmatrix} \left(\omega\theta_{xlas} \cdot \frac{\partial V_x}{\partial \theta_{xlas}} \right)^2 & \left(\omega\theta_{ylas} \cdot \frac{\partial V_x}{\partial \theta_{ylas}} \right)^2 \\ \left(\omega\theta_{xlas} \cdot \frac{\partial V_y}{\partial \theta_{xlas}} \right)^2 & \left(\omega\theta_{ylas} \cdot \frac{\partial V_y}{\partial \theta_{ylas}} \right)^2 \\ \left(\omega\theta_{xlas} \cdot \frac{\partial V_z}{\partial \theta_{xlas}} \right)^2 & \left(\omega\theta_{ylas} \cdot \frac{\partial V_z}{\partial \theta_{ylas}} \right)^2 \end{bmatrix} = (1 \times 10^{-2}) \begin{bmatrix} 0.000257 & 0.000778 \\ 0.1238 & 0.3747 \\ 6.1961 & 18.76 \end{bmatrix} \quad (138)$$

7.5.4 Component Contributions to Total Uncertainty

Once the average values for the individual terms in the uncertainty equation given in equation 52 were calculated, these values were used to calculate an average uncertainty for each velocity component. The average values for the uncertainty of each velocity component were: $\omega V_x = 14.076$ m/s, $\omega V_y = 32.743$ m/s, and $\omega V_z = 3.562$ m/s. The average values used in equation 52 were also used to determine how much each term contributed to the total uncertainty of the velocity measurement. Table 7.1 shows a breakdown in terms of percentage, that each term contributed to the total uncertainty for the V_x velocity component. Table 7.2 shows a breakdown in terms of percentage, that each term contributed to the total uncertainty for the V_y velocity component. Table 7.3 shows a breakdown in terms of percentage, that each term contributed to the total uncertainty for the V_z velocity component. Looking at tables 7.1, 7.2, and 7.3, the largest contributors to the total uncertainty of the V_x , V_y , and V_z velocity component are, by far, the changes in optical frequency

measured by the VT DGV system. The other uncertainties in this calculation are miniscule compared to the uncertainties in the measured changes in optical frequency.

Table 7.1: Uncertainty Contribution Percentages for V_x velocity uncertainty.

	ωV_x
Δv_1	20.12086%
Δv_2	28.29034%
Δv_3	51.54705%
WN	0.00000%
θ_{x1}	0.00005%
θ_{x2}	0.00970%
θ_{x3}	0.00832%
θ_{y1}	0.00168%
θ_{y2}	0.00576%
θ_{y3}	0.02048%
θ_{xlas}	0.00005%
θ_{ylas}	0.00005%

Table 7.2: Uncertainty Contribution Percentages for V_y velocity uncertainty.

	ωV_y
Δv_1	89.83588%
Δv_2	1.58670%
Δv_3	0.30193%
WN	0.00000%
θ_{x1}	0.00022%
θ_{x2}	0.00054%
θ_{x3}	0.00138%
θ_{y1}	0.00751%
θ_{y2}	0.00032%
θ_{y3}	0.00340%
θ_{xlas}	0.00001%
θ_{ylas}	0.00001%

Table 7.3: Uncertainty Contribution Percentages for V_z velocity uncertainty.

	ωV_z
Δv_1	8.04532%
Δv_2	88.94762%
Δv_3	0.98498%
WN	0.00000%
θ_{x1}	0.00002%
θ_{x2}	0.03052%
θ_{x3}	0.00016%
θ_{y1}	0.00067%
θ_{y2}	0.01812%
θ_{y3}	0.00039%
θ_{xlas}	0.00076%
θ_{ylas}	0.00076%

The results from this uncertainty analysis indicate that future work on the VT DGV system needs to focus on reducing the uncertainties in the measured changes in optical frequency. Looking at the uncertainties of the transmission ratios used to calculate the change in optical frequency for each camera module, found in section 7.5.1, the uncertainties for the transmission ratios in the data area are all over 3.5 times greater than the uncertainties of the laser reference transmission ratios for each camera module, so, the uncertainties for the transmission ratios in the data plane contributed the largest portion to the total uncertainty in the measured changes in optical frequency. The uncertainties in the transmission ratios from the data area were directly affected by the poor performance of the Nd:YAG laser and by the fact that only seven calibration wheel images were reduced. If the laser performance was more stable and if more of the calibration wheel images could have been reduced, this would have significantly reduced the uncertainties from the measured change in optical frequency.

Improving the technique used to measure the laser reference transmission ratio would also help to reduce the uncertainties of the measured changes in optical frequency. The technique used to measure the laser reference transmission ratio can be improved upon by adding a fourth camera to the VT DGV system, and using this camera to monitor the spatial and temporal variations in the laser pulses used to acquire velocity data. This improvement would be two fold. First, it would allow

spatial variations within a given laser pulse to be measured and accounted for. Adding a fourth camera would also increase the number of pixels used to calculate the laser reference transmission ratio, thus reducing the uncertainty of this value.